




Effect of supersaturation on the oral bioavailability of paclitaxel/polymer amorphous solid dispersion

Linlin Miao¹ · Yuheng Liang¹ · Wenli Pan¹ · Jingxin Gou¹ · Tian Yin² · Yu Zhang¹ · Haibing He¹ · Xing Tang¹ 

Published online: 5 September 2018
© Controlled Release Society 2018

Abstract

The aim of the present investigation was to evaluate the effect of supersaturation on the oral absorption of paclitaxel (PTX) *in vivo*. To achieve this, a PTX amorphous solid dispersion (ASD) was prepared by the solvent cast method. Among the enteric polymers tested, hypromellose acetate succinate (HPMCAS) MF was found to be the most suitable polymer for maintaining PTX supersaturation and inhibiting crystallization *in vitro*. The dissolution rate and extent of the ASD was remarkably improved compared with a physical mixture (PM) of PTX, HPMCAS-MF, and Poloxamer 188 (F68), reaching an apparent drug concentration of 25–30 µg/mL and maintaining it for more than 2 h. The liquid–liquid phase separation (LLPS) concentration of PTX in the presence of HPMCAS-MF was determined to be 23 µg/mL, which was different to that of 40 µg/mL in the absence of polymer. It indicated that HPMCAS was substantially incorporated into the drug-rich phase. Also, HPMCAS could adsorb to the PTX surface and provided an interfacial barrier for crystal growth, as well as retard the incorporation of PTX from solution into the growing crystal lattice. The results of X-ray diffraction, differential scanning calorimetry analysis, and transmission electron microscopy confirmed that PTX existed in the amorphous state in the solid dispersion. Compared with the PM group, the ASD prepared with HPMCAS-MF and F68 achieved a 1.78-fold increase in relative oral bioavailability, while PTX solution yielded a 1.56-fold increase, which could be explained that the solubility and the permeability of PTX were not increased simultaneously through supersaturation *in vivo*. Likely, it was because Cremophor inhibited P-glycoprotein in the intestine to some extent and maintained PTX at a higher concentration for a longer time.

Keywords Supersaturation · Bioavailability · Amorphous solid dispersion · Polymer · PTX

Introduction

Oral delivery is the most common and convenient delivery system, with advantages such as reduced side effects and improved patient compliance [1]. However, there is a big challenge for the oral delivery of BCS IV drugs, which are classed with poor solubility and permeability. A lot of strategies have been investigated to solve the solubility problem, such as the application of micelles, liposomes, emulsions, nanoparticles, solid dispersions, etc. However, for cyclodextrin-, surfactant-,

micelle-, and cosolvent-based formulations and more, the increase of the apparent solubility always comes with a failure to improve the overall absorption for the decreased permeability [2–4]. The mathematical equation describing membrane permeability suggests that solubility and permeability relate closely, with an apparent certain interplay between them. As opposed to other solubilization methods, amorphous solid dispersions could increase the apparent solubility of drugs by allowing them to achieve and maintain supersaturation, rather than through changing the equilibrium solubility of the drug [5].

Paclitaxel (PTX) is an effective antineoplastic agent and has been widely used to treat breast, ovarian, non-small lung, and hormone refractory prostate cancers [6]. The commercial product of PTX, Taxol®, is composed of 30 mg drug dissolved in a 50/50 (v/v) mixture of Cremophor EL/dehydrated ethanol, which is further diluted in isotonic saline solution before intravenous administration [7]. Unfortunately, a series of adverse effects are associated with *i.v.* administration of

✉ Xing Tang
tanglab@126.com

¹ Department of Pharmaceutics, School of Pharmacy, Shenyang Pharmaceutical University, No. 103 Wenhua Road, Shenyang 110016, China

² School of Functional Food and Wine, Shenyang Pharmaceutical University, No. 103 Wenhua Road, Shenyang 110016, China

Cremophor EL, such as acute hypersensitivity reactions, hyperlipidaemia, neurotoxicity, and more [5, 8]. The oral bioavailability of PTX is very low mainly due to its poor solubility [6], CYP3A4-mediated pre-systemic metabolism, P-glycoprotein drug efflux pumps, and poor drug dissolution in the gastrointestinal tract. Nanoengineered systems have been successfully explored in multifarious ways to improve the oral delivery of PTX, such as nanoparticles [9], polymeric micelles [8, 10], nanocrystals [11, 12], chitosan-PTX conjugates [13], layerosomes [14], self-emulsifying drug delivery systems [15], lipid nanocapsules [16], etc. The absorption and oral bioavailability of PTX can be enhanced through the inhibition of the P-glycoprotein (P-gp) efflux system and cytochrome P450 metabolism, by opening the junctions and bypassing the efflux pump, via endocytosis and active endocytic processes, or by extending the gastrointestinal tract residence time.

Pluronic block copolymers containing hydrophilic poly(ethylene oxide) (PEO) blocks and hydrophobic poly(propylene oxide) (PPO) blocks have been found to inhibit P-gp efflux and reverse the MDR effect [17]. Besides, Pluronic block copolymers L81, P85, and F68 have been shown to restrain the intestinal secretion of lipoproteins [1], which can be used to deliver oral lipophilic drugs, particularly those which are substrates for P-gp efflux. Also, it has been reported that F68-based solid dispersions could improve the dissolution of docetaxel, and that there exists certain intermolecular interactions between docetaxel and poloxamer [18].

ASD can be used to improve the oral bioavailability of drugs with poor water solubility, due to the excipients acting to prevent the nucleation and growth of the crystalline drug from the supersaturated solution phase [19]. The induced supersaturation can enhance drug absorption via an increase in thermodynamic activity and free drug concentration [7], resulting in a saturation of P-gp. Whereas, when the apparent solubility is higher than the equilibrium solubility of the drug, there is a trend for the drug to precipitate and drug absorption may then be compromised. Alternatively, liquid–liquid phase separation (LLPS) occurs, whereby a metastable equilibrium exists between free drug in the bulk aqueous solution (drug-poor phase) and a non-crystalline, water-saturated, drug-rich phase [20]. The key point is to choose the ideal excipient to delay the onset of crystallization. Drug/HPMCAS spray-dried dispersions were shown to be more effective at achieving and maintaining supersaturation of eight low-solubility drugs of widely varying structure *in vitro* than 40 other materials tested [21]. Zelboraf® (Roche), an amorphous solid dispersion of vemurafenib-hypromellose acetate succinate (30:70, *w/w*), is one of three commercialized oncology formulations containing a solid dispersion. The dissolution is approximately 30 times higher than that of crystalline vemurafenib and the plasma concentration is almost 5 times of vemurafenib [22]. Amidon et al. [23] stated that permeability and solubility are

the fundamental parameters controlling oral drug absorption. Amorphous solid dispersions are usually used to improve the bioavailability of BCS II classic drug [24–26], and there is rare research on BCS IV drugs. Still, it has been reported that the solubility and the permeability of rifaximin were increased simultaneously via a rifaximin amorphous solid dispersion. Even though the drug is a BCS class IV (low-solubility, low-permeability) drug and also a P-gp substrate, permeability could be increased in the high supersaturation level as a result of efflux transporter saturation [27]. As well, amorphous rifaximin could achieve a 5-fold higher systemic bioavailability compared with another polymorphs [28]. The low oral bioavailability is still hampered by the combination of intestinal efflux and pre-systemic metabolism, even with a relatively high permeability in Caco-2 cells from apical to basolateral [29]. It was reported that the luminal PTX concentration could be enhanced by increasing solubility and dissolution rate, which will further efficiently saturate the intestinal efflux and/or metabolism of PTX [30–32]. Potentially, it is possible to improve the bioavailability of PTX through saturating the intestinal P-gp efflux and cytochrome P450 3A4 metabolizing enzymes as it exhibits high efflux (Fig. 1) [33–35].

The aim of the present research was mainly to develop amorphous solid dispersion of PTX to investigate the impact of supersaturation on the *in vivo* bioavailability. To achieve this, PTX solid dispersions were prepared with enteric polymers and F68, and the dissolution was evaluated under non-sink conditions. Furthermore, the impact of the polymers on the LLPS values in PBS was assessed to better understand factors impacting the dissolution behaviors and longevity of supersaturation following dissolution of the ASDs. HPMCAS-MF was found to be the most suitable excipient to prolong supersaturation of PTX via preventing drug crystallization and retard precipitation. The solid-state properties of ASDs were further evaluated by differential scanning calorimetry (DSC), Fourier transform infrared spectroscopy (FT-IR), X-ray diffraction (XRD), and transmission electron microscopy (TEM). Furthermore, pharmacokinetics and stability study of the solid dispersions were also performed. In general, this work revealed the potential effects of supersaturation on the intestinal absorption of PTX amorphous solid dispersion.

Materials and methods

Materials

The following materials were purchased from the companies stated and used as received. PTX was purchased from Shanghai Sunve Pharma Co. Ltd. (Shanghai, China), HPMCAS (LF, MF, HF) was obtained from Ashland Specialty Ingredients (Wilmington, USA), and Poloxamer 188 (Pluronic F68) was obtained from BASF AG

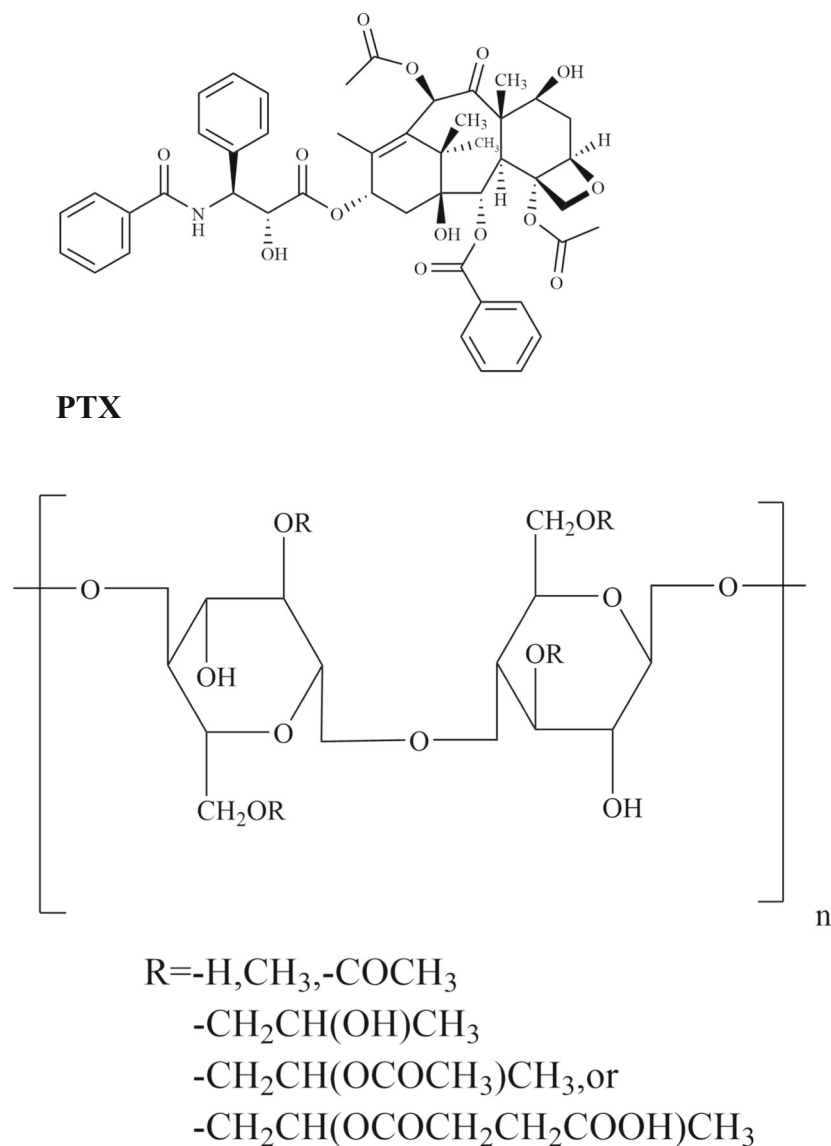


Fig. 1 Chemical structures of paclitaxel (PTX), hydroxypropylmethylcellulose acetate succinate (HPMCAS), and poloxamer 188 (F68) and schematic presentation of the solid dispersion in the intestine

(Ludwigshafen, Germany). All buffer salts used for dissolution medium were purchased from Tianjin Kermer Chemical Reagent Co., Ltd. (Tianjin, China). The solvents used in the experiments were obtained from Tianjin Concord Technology Co. Ltd. (Tianjin, China). All other reagents were of analytical grade and used without further purification.

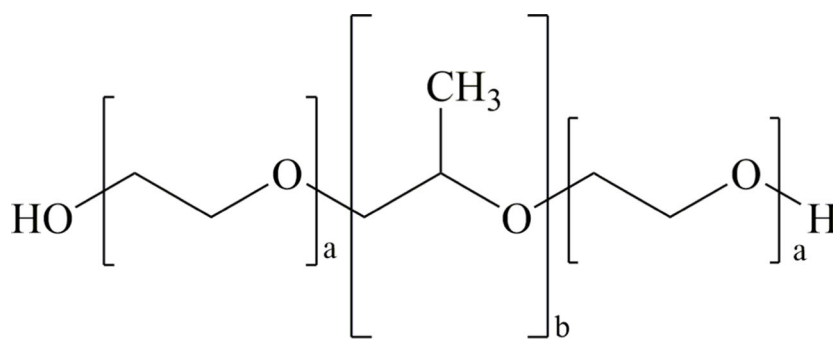
Preparation of PTX SDs

PTX ASDs with 10% drug loading were prepared through the solvent casting method. In brief, PTX and enteric polymer with or without F68 were dissolved separately in ethanol/acetone (1:1 (v/v) ratio) cosolvent. The two solutions were then mixed together and stirred for 5 min. Finally, the solution

was spread into a petri dish and allowed to evaporate at 60 °C for 24 h until complete removal of solvent. The resulting films were pulverized, ground by a frozen grinding machine (JXFSTPRP-CL-48), and conserved in a desiccator at room temperature until further evaluation (Table 1).

Determination of apparent solubility

Solubility of crystalline PTX in a 50 mM phosphate-buffered solution (PBS, pH 6.8) in the presence of either HPMCAS-MF or F68 or the combination of the two was determined by stirring an excess amount of crystalline drug in the dissolution medium, followed by sonication for 10 min and then shaking using an orbital shaker (37 °C, Burrell wrist action shaker,



F68

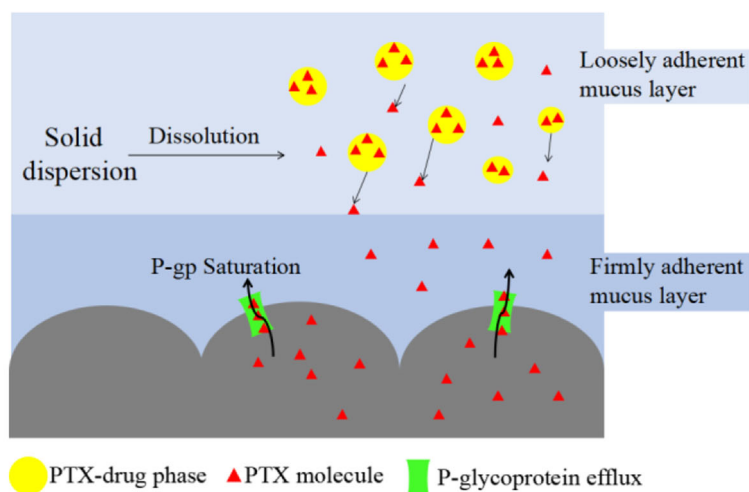


Fig. 1 continued.

model 75) for 48 h. The suspensions were subsequently centrifuged at 12,000 rpm (HC-3018R High speed refrigerated centrifuge, Anhui, Zonkia Scientific Instruments Co., Ltd) for 15 min, and the drug concentration in the supernatant was determined by HPLC. The concentration of HPMCAS-MF or F68 was 0.5, 1, or 3 mg/mL. The quantification of PTX was performed according to previously described methods

[36, 37]. The equilibrium solubility of PTX was also determined in the presence of 0.01, 0.05, and 0.1% (*w/v*) Cremophor RH40 in 50 mM at pH 6.8 PBS using the method outlined above.

UV spectroscopy was used to determine the amorphous solubility of PTX. The samples analyzed consisted of 100 mL PBS (50 mM, pH 6.8) stirred at 300 rpm and

Table 1 The composition (*w/w*) of PMs (physical mixtures) and SDs (solid dispersions)

Formulation	HPMCAS-LF	HPMCAS-MF	HPMCAS-HF	HPMCP-55	L100	F68	PTX
PM1		75				15	10
PM2		90					10
SD1		75				15	10
SD2	75					15	10
SD3			75			15	10
SD4				75		15	10
SD5					75	15	10
SD6		90					10

HPMCAS, hypromellose acetate succinate (LF/MF/HF mean different grades of HPMCAS); HPMCP-55, hydroxypropylmethyl cellulose phthalate; L100, Eudragit® L100; F68, poloxamer 188; PTX, paclitaxel

maintained at 37 °C using a jacketed vessel fed by a Julabo MA water bath (Seelbach, Baden-Wurttemberg, Germany), with or without dissolved polymer. The polymer HPMCAS-MF was added at 450 and 32 µg/mL, and HPMCP and L100 were added at 450 µg/mL. PTX was dissolved in dimethyl sulfoxide (DMSO) at a concentration of 10 mg/mL. Through the use of a syringe pump (KD Scientific KDS 220 multi-channel syringe pump, USA), the solution was continuously added to the buffer at an infusion rate of 0.12 mL/min. Approximately, 0.6 mL DMSO was added to the aqueous medium, and less than 1% DMSO has been confirmed not to influence the solubility of PTX. Light scattering was detected (iDH 2000-UV, Shanghai Ideaoptics Co.Ltd) by monitoring the extinction at a non-absorbing wavelength of 400 nm. To assess the impact of Cremophor RH40 on the degree of supersaturation, the amorphous solubility of PTX was measured in the presence of three different concentrations of Cremophor RH40, with one concentration below the critical micelle concentration (CMC) and the other two above the CMC. A 20-mg/mL PTX stock solution was added to the PBS at a rate of 0.2 mL/min to rapidly obtain the LLPS concentration prior to crystallization occurring.

When LLPS occurred, the baseline signal increased sharply due to the formation of scattering species. The concentration where the extinction increased for each system was estimated by fitting the data in the regions of low and high extinction using linear regression analysis and determining the intersection of the two curves. LLPS onset concentration represents the amorphous solubility to some extent. The degree of supersaturation can be calculated using the following equation [7]:

$$S = \frac{C}{C_{eq}}$$

where S is the supersaturation ratio, C is the experimental free drug concentration, and C_{eq} is the equilibrium solubility of the crystalline drug. When the supersaturation ratio is higher than 1, there is a trend for the drug solution to produce liquid-liquid phase separation or drug crystallization.

In vitro dissolution under non-sink condition

The dissolution profiles of pure PTX powder, PMs, and SDs were evaluated in non-sink dissolution condition, which can facilitate the evaluation of the degree of supersaturation. Briefly, PTX powder, PMs, or SDs containing 3 mg PTX were transferred into 50 mL PBS and the instrument was set to 200 rpm at 37 °C. At pre-determined time points (15, 30, 45, 60, 90, and 120 min), 3 mL sample was withdrawn and replaced with the same volume of PBS. The samples were filtered with 0.45 µm syringe filters, and then analyzed by HPLC.

In order to assess the abilities of HPMC-AS and F68 to maintain the solution supersaturation of PTX, different concentration solutions of HPMC-AS and F68 were prepared. A PTX solution in DMSO was prepared at 10 mg/mL, of which 100 µL was added to 20 mL of PBS pre-dissolved with various excipients. The solution was then vibrated at a frequency of 200 rpm. After 20 min, 1 h, 2 h, and 4 h, 1 mL solution was withdrawn and centrifuged at 12,000 rpm for 10 min. The obtained clear supernatant was subsequently analyzed by HPLC.

Characterization of SDs

Differential scanning calorimetry

A differential scanning calorimeter (DSC-60 SHIMADZU) was used to produce and analyze thermograms of each sample. Approximately 5 to 10 mg samples (PTX, SD1, SD6, PMs, and HPMCAS) were weighed into an aluminum pan and heated from ambient temperature to 300 °C at a heating rate of 10 °C/min. A nitrogen flow rate of 40 mL/min was used during each run.

Fourier transform infrared spectroscopy

FT-IR spectra of the SD1, SD6, HPMCAS, PTX, F68, and PMs were collected by Fourier transform infrared spectroscopy (Vertex 70, Bruker Optics, Ettlingen, Germany) with a spectral resolution of 4 cm⁻¹. The IR spectra in the wave number range 4000–400 cm⁻¹ were recorded for further comparison.

Power X-ray diffraction analysis

Power X-ray diffraction (PXR) analysis was also used to ascertain the existing state of PTX in the PTX solid dispersion. X-ray powder diffraction measurements were performed on a D8 Advance X-ray diffractometer (Bruker, Karlsruhe, Germany). Samples of approximately 0.5 mm thickness were placed in a metal sample holder, placed in the diffractometer, and scanned at a current of 40 mA and a voltage of 40 kV. The scan range was 5–60° (2θ), with a scan speed of 4°/min.

Transmission Electron microscopy

TEM experiments and electron diffraction of SD1 and SD6 were performed using a JEM-2100 transmission electron microscope (JEOL, Japan) with an accelerating voltage of 200 kV. Samples were prepared by dropping the diluted solution with corresponding polymer and PTX onto a 230-mesh copper TEM grid with carbon film, followed by heating to 60 °C to remove residual solvent. Electron diffraction was used to confirm if there was crystallinity in the solid dispersions.

Stability study

In order to investigate the stability of SD1 and SD6, the samples were stored at 40 °C with 75% relative humidity for 1 month. DSC and XRD were examined to evaluate the crystallinity of PTX. The dissolution profiles were conducted by the method described in section “[In vitro dissolution under non-sink condition.](#)”

In vivo pharmacokinetic evaluation

In vivo protocol

Twenty-four male Sprague-Dawley rats weighing 180–200 g were provided by the Experimental Animal Center of Shenyang Pharmaceutical University. Animals were fasted overnight before experiments. All animal studies were carried out in compliance with the Guideline for Animal Experimentation approved by the Animal Ethics Committee of the institution. Rats were randomly divided into the following four groups ($n = 6$): (1) SD1 treatment group, (2) SD6 treatment group, (3) PTX solution (PTX-sol) treatment group, and (4) PM1 treatment group. The PTX-sol was prepared by dissolving 50 mg PTX in a mixed solvent (2.485 mL ethanol + 2.635 mg Cremophor® RH40), and then the solution was diluted to a concentration of 2 mg/mL. The PTX oral formulations were administrated at a single dose of 20 mg/kg. Blood samples (0.3 mL) were collected via the orbital venous plexus at 15 min, 30 min, 1 h, 2 h, 4 h, 6 h, 8 h, 12 h, and 24 h after administration. After centrifugation at 6000 rpm for 10 min, the obtained plasma was stored at -20 °C until required for analysis.

Plasma samples (100 μ L) were mixed thoroughly with 20 μ L of a 5- μ g/mL DTX solution and vortexed for 3 min and then extracted with 2.5 mL tert-butyl methyl ether (TBME) and followed by vortexing for 10 min. After centrifugation at 4000 rpm for 10 min, 2 mL supernatant was removed and evaporated to dryness at 40 °C with a gentle stream of nitrogen. After, 100 μ L of acetonitrile was added followed by vortexing for 10 min, and then centrifugation at 12,000 rpm for 10 min. Finally, 85 μ L aliquots were transferred for determination.

LC-MS analysis of PTX in plasma

Analytic separation was achieved on an ACQUITY Ultra-Performance Liquid Chromatography system (Waters Corp., Milford, MA, USA) using an XBridge™ C18 column (75 \times 4.6 mm, 2.5 μ m, Waters Corp., Milford, MA, USA). Mobile phases A and B consisted of acetonitrile and H₂O/formic acid 99.9:0.1 (V/V). The gradient (0.2 mL/min) was performed as follows: starting at 50% A and reaching linearly to 90% A in 0.9 min. This was followed by 1.4 min at 90% A, then

reaching linearly to 50% A in 0.2 min. Finally, equilibrate 0.5 min at 50% A. The column temperature was held at 35 °C.

Quantitative determination of PTX was performed with a Waters ACQUITY™ XEVOTQ mass spectrometer. Data was acquired in electrospray ionization (ESI) mode with positive ion detection and multiple reaction monitoring (MRM). A cone voltage of 10 V and capillary voltage of 3.00 kV were used. The desolvation temperature was maintained at 400 °C and nitrogen was used as the desolvation gas with a flow rate of 550 L/h. The MS/MS transition of PTX was 854.40 \rightarrow 569.2 and that of docetaxel was 808.48 \rightarrow 527.3. The mass spectrometric data were collected using the Masslynx™ NT4.1 software (Waters Corp., Milford, MA, USA) and analyzed by the QuanLynx™ program (Waters Corp., Milford, MA, USA).

Pharmacokinetic data analysis

The plasma concentration of PTX vs. time profile was analyzed by a two-compartmental method using DAS 2.0 software (Mathematical Pharmacology Professional Committee of China, Shanghai, China). The PK parameters were analyzed for statistical significance with an unpaired Student's *t* test, with a significance level of $P < 0.05$.

Results and discussion

Apparent solubilities of PTX

The aqueous solubility of crystalline PTX in the presence or absence of HPMCAS(MF), F68, and/or Cremophor RH40 is summarized in Table 2.

Without HPMCAS (MF) or F68, the aqueous solubility of crystalline PTX in PBS at 37 °C is very low at 0.3 μ g/mL.

Table 2 Apparent solubility of PTX in the presence and absence of polymers at 37 °C ($n = 3$)

Solvent	Solubility (μ g/mL)
PBS (pH 6.8)	0.30 \pm 0.02
HPMCAS	
0.5 mg/mL	0.33 \pm 0.05
1 mg/mL	0.26 \pm 0.03
3 mg/mL	0.31 \pm 0.04
F68	
0.5 mg/mL	0.19 \pm 0.02
1 mg/mL	0.20 \pm 0.03
3 mg/mL	0.24 \pm 0.03
HPMCAS	
0.5 mg/mL + F680.1 mg/mL	0.37 \pm 0.03
2.5 mg/mL + F680.5 mg/mL	0.32 \pm 0.04
Cremophor RH40	
0.01%	0.28 \pm 0.15
0.05%	1.20 \pm 0.18
0.10%	1.93 \pm 0.10

With the addition of HPMCAS up to 2.5 and 0.5 mg/mL F68, the solubility of PTX remained unchanged, indicating that the coexistence of HPMCAS and F68 had a negligible effect on the solubility of PTX. The equilibrium solubility of PTX increased ~ 4 times to 1.20 $\mu\text{g}/\text{mL}$ with 0.05% Cremophor RH40 and to 1.93 $\mu\text{g}/\text{mL}$ with 0.10% Cremophor RH40.

The amorphous solubility of PTX or the concentration where LLPS occurred was determined by UV spectroscopy. Piao et al. [38] reported that the theoretical solubility ratio of amorphous/crystalline PTX was 92.6 (37 °C). According to Fig. 2a, the LLPS concentrations of PTX in the presence of the polymers (HPMCP-55 and L100) were found to be similar to the LLPS concentration in the absence of polymer, which was approximately 40 $\mu\text{g}/\text{mL}$, implying that HPMCP-55 and L100 did not change the thermodynamic activity of the drug-rich phase [39]. However, for a solution of PTX with HPMCAS (MF), it is apparent that there was a decreased extinction concentration of approximately 23 $\mu\text{g}/\text{mL}$. This was in agreement with an example of danazol where LLPS

occurred at lower concentrations with low concentrations of added polymers (PVP, HPMC, HPMCAS) [40]. Chen et al. found that the amorphous precipitates contained ~ 16 wt% of HPMC-AS [41]. Furthermore, solution ^1H NMR measurements revealed that the polymer was distributed to the drug-rich phase during LLPS. With more polymer incorporated and the more the hydrophobic nature of the polymer, the supersaturation solution was found to be more stable [42]. Also, the reduction of LLPS concentration further indicated that HPMCAS was substantially incorporated into the drug-rich phase, namely that there existed some interactions between HPMCAS and PTX. The FT-IR 1600–1800 cm^{-1} spectra of HPMCAS and PTX are similar, and there exists strong intermolecular hydrogen bonding and hydrophobic interactions between HPMCAS and PTX, as both have carbonyl and hydroxyl groups. HPMCAS is likely localized on the surface of the colloidal particles due to its negative charge under alkaline conditions [43, 44]. The zeta potential of PBS with only HPMCAS was -3.02 mV while that was -12.4 mV in the

Fig. 2 **a** UV extinction intensity of PBS with or without polymer. **b** The visual examination of four supersaturated solutions after 48 h at ambient temperature. **c** Crystal habit of precipitations from the PTX supersaturation solution; top, solution without polymer. **d** UV extinction intensity of PBS with different concentrations of Cremophor RH40

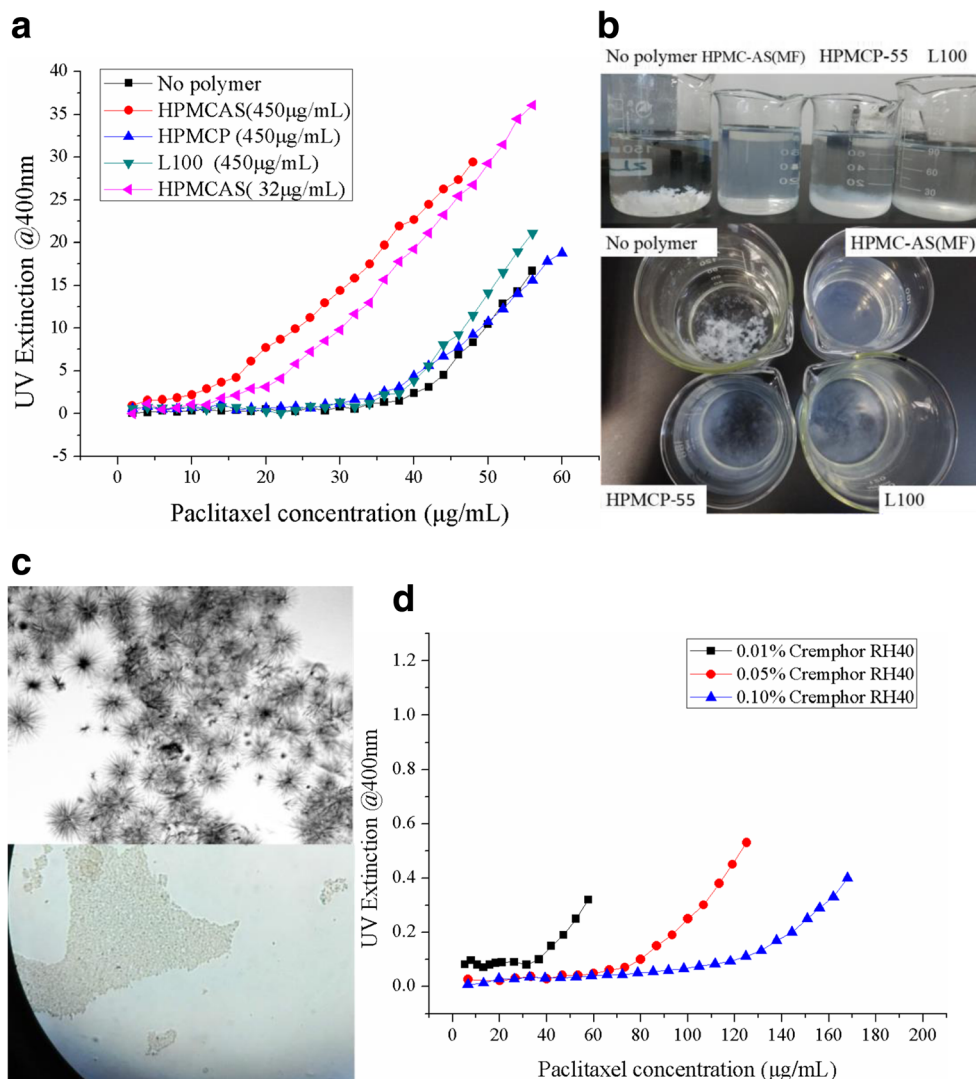


Table 3 Particle size (diameter, nm) for PTX systems at a concentration above the LLPS concentration with various polymers, comparing the effect of pre-dissolved additives (HPMCAS-MF, HPMCP-55, L100) on the PTX colloidal aggregates produced using the solvent-shifting method

	HPMCAS-MF	HPMCP-55	L100
Particle size (nm)	250.3 ± 115.4	224.4 ± 106.1	266.0 ± 141.8

The polymer concentration was 450 µg/mL

supersaturated solution with HPMCAS, which further serves as an indication of adsorption of HPMCAS at the drug-rich phase interface (data not shown). Besides, the hydrophobic regions of HPMCAS could provide sites for PTX association, while hydrophilic areas play the role of stabilizing the drug-rich phase [21]. Potentially, HPMCAS reduced the activity of PTX and further lead to a decreased concentration where LLPS occurred. Further, the concentration of HPMCAS had no significant influence on the LLPS concentration.

UV extinction experiments revealed that LLPS occurred at 40, 82, and 125 µg/mL in 0.01, 0.05, and 0.1% Cremophor RH40 solutions, respectively, as compared with that at 40 µg/mL in buffer (Fig. 2d). It was observed that increasing the Cremophor RH40 concentration led to enhanced solubility and a corresponding increase in LLPS concentration [45].

After the addition of PTX solution, there appeared obvious precipitation in the solution without added polymer. The solution with 450 µg/mL polymers was completely homogeneous with a slight bluish color, characteristic of the presence of a second scattering phase. Four hundred fifty micrograms per milliliter is the concentration of the polymer that would be present in the solution following a complete dissolution of the PTX solid dispersions. The particle sizes of the colloidal droplets were determined with dynamic light scattering (DLS). The average sizes of the drug-rich phase obtained by the antisolvent addition method with or without polymer are comparable (Table 3). Both the UV extinction and DLS data were consistent with the formation of a second phase which scattered light. After 48 h, it could be seen that only HPMCAS solution was still homogeneous, whereas HPMCP-55 solution had

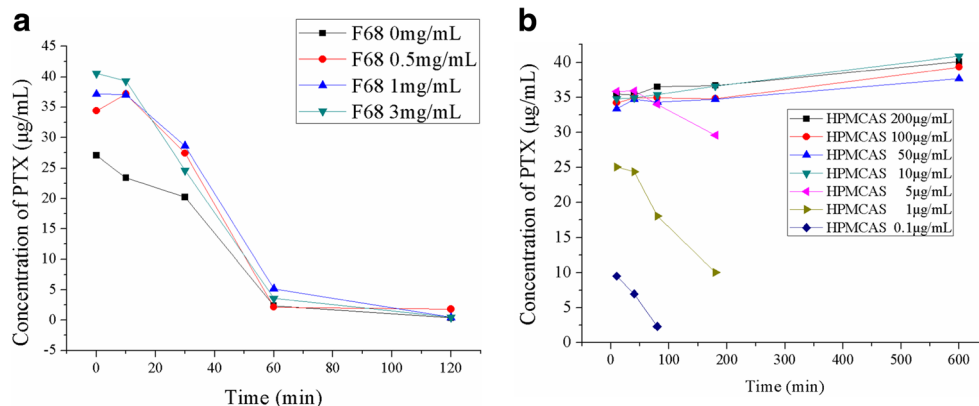
precipitated and the L100 solution was observed to be cloudy. A higher maximum supersaturation with HPMCP or L100 led to a sharper decline in supersaturation caused by rapid precipitation [46]. The phenomenon was consistent with the outcome that LLPS occurred at a lower concentration with the presence of HPMCAS, as the supersaturation level was reduced, and thus the supersaturation solution was less susceptible to precipitation [47]. That is, HPMCAS could influence the supersaturation of a solution in both thermodynamic and kinetic ways [48]. However, HPMCP and L100 could only be involved in the kinetics of precipitation, inhibiting crystallization in some way.

As is shown in Fig. 2c, compared with the crystalline particles formed in the presence of polymers, the crystalline particles formed in the absence of polymer present a random needle-like habit composed by crystalline agglomerates, which was caused by rapid and high supersaturation. Supersaturation must exceed a critical supersaturation, after which the secondary nucleation appears in the crystallographic z-axis, namely the “birth and spread” growth mechanism [49]. Additives HPMCP and L100 did modify the crystal morphology at the macroscopic scale, which showed in part that they could impede the growth of specific crystal faces. In summary, HPMCAS (MF) was the most appropriate enteric polymer to prevent crystallization and maintain supersaturation of PTX.

The effect of HPMC-AS or F68 on PTX supersaturation maintenance

As shown in Fig. 3, F68, regardless of its concentration, is not effective in maintaining PTX supersaturation. The precipitation was in an amorphous state under a polarization microscope (data not shown). In contrast, HPMCAS significantly prolonged PTX supersaturation in PBS with a PTX concentration of 35 µg/mL. The concentration was higher than the LLPS concentration, as some tiny colloidal aggregates could not be completely eliminated by high-speed centrifugation. The later increased concentration of PTX may be caused by the loss of solvent. HPMCAS of 10 µg/mL concentration was sufficient to keep PTX at a supersaturation state. As well, the maintenance

Fig. 3 Supersaturation of PTX solutions in the presence of different amounts of **a** F68 or **b** HPMCAS. The initial drug concentration was 50 µg/mL. Note: The concentration of 50 µg/mL is not an experimentally measured value but represents the theoretical starting concentration calculated based on the amount of PTX DMSO solution added



time of the supersaturation was related with the concentration of HPMCAS-MF. The solutions gradually appeared to precipitate with an increase in polymer concentration.

In vitro dissolution testing

Figure 4 shows the in vitro dissolution behaviors of PTX solid dispersions prepared with various polymers and PTX-sol under non-sink condition. Dissolution results indicated that F68 had no obvious effect on the dissolution rate and extent of PTX from the solid dispersion, which was consistent with the supersaturation maintenance of F68. Compared with HPMCP-55, L100, HPMCAS-LF, and HPMCAS-HF, HPMCAS-MF was the best polymer, introducing a fast dissolution rate and could maintain PTX at a steady concentration without decreasing. The solutions with SD1 and SD6 turned to slight bluish during the dissolution process, demonstrating the appearance of liquid–liquid phase separation. When the PTX concentration was at amorphous solubility, the supersaturation ratio was almost 77. The solid dispersion with HPMCAS-LF had the fastest dissolution rate, but the concentration decreased sharply. It should be noted that the cumulative release percentage of PTX approximately accounted for 50% of the total drug dose, as part of the PTX was in the aggregations caused by LLPS and the dissolution was in non-sink conditions. For PTX-sol, PTX was incorporated into surfactant micelles, and so the concentration only changed with the removal of dissolution medium.

XRD, DSC, FT-IR, and TEM

X-ray diffraction spectra, DSC thermograms, and FT-IR spectra were used to characterize the state of PTX in the physical

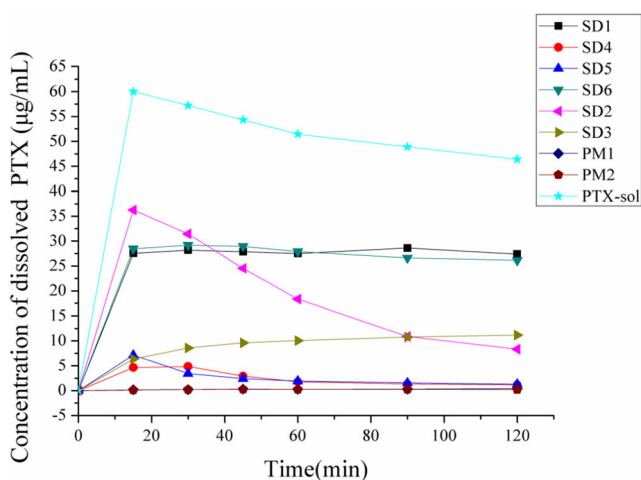


Fig. 4 Dissolution performance of PTX solid dispersions prepared with PTX and various polymers. Drug loading was 10% with HPMCAS (LF, MF, and HF), HPMCP-55, and L100. Dissolution was carried out using the small-scale dissolution test in 50 mL PBS (50 mmol/L, pH 6.8) at 37 °C

mixtures and solid dispersion, and the results are shown in Fig. 5. The sharp diffraction peaks of pure PTX indicated the crystalline phase. F68 showed two diffraction peaks at

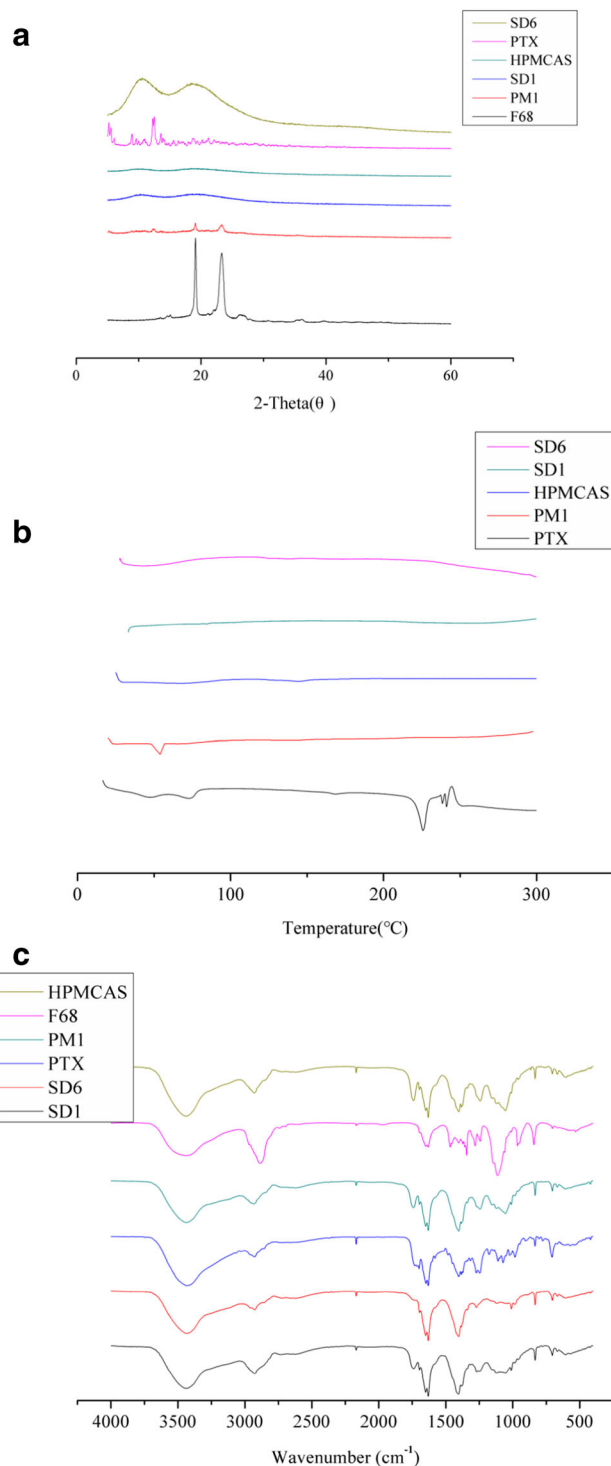


Fig. 5 X-ray diffraction spectra (a), DSC thermograms (b), and FT-IR spectra (c) of PTX formulations and their components. PM1 (HPMCAS-MF/F68/PTX = 75:15:10). PTX-SD1 (HPMCAS-MF/F68/PTX = 75:15:10) and SD6 (HPMCAS-MF/PTX = 90:10). PTX, paclitaxel; HPMCAS, HPMCAS-MF

diffraction angles of (2θ) 19.14° and 23.25°. The PM showed sharp peaks at a diffraction angles (2θ) of 12.25°, 19.14°, and 23.31°, indicating that PTX and carriers were all in crystalline forms. No crystalline peaks of PTX were found in the solid dispersion, and broad and featureless PXRD patterns suggested that PTX in the solid dispersion was molecularly dispersed in an amorphous state.

The DSC thermograms (Fig. 5b) confirmed the results of the XRD analysis. Physical mixtures only had one visible endothermic peak at 55 °C, which was the characteristic peak of F68. An exothermic peak could be observed following the endothermic melting peak of PTX due to its degradation. The absence of the melting peak of PTX in the two solid dispersions and the PM1 indicated that PTX may be present in an amorphous state.

FT-IR spectra can be used to determine whether there is any interaction between the drug and the polymer in the solid state. FT-IR spectra of 2000–1500 cm^{-1} of PTX, HPMCAS, PMs, and SDs were almost the same except for an intensity difference. PTX had a peak at 1733 cm^{-1} , while HPMCAS had a peak at 1740.6 cm^{-1} . For the physical mixtures, the peak was at 1740.3 cm^{-1} , same as HPMCAS alone. In the PTX-HPMCAS solid dispersion system, the carbonyl peak showed a red shift from 1740 to 1737.7 cm^{-1} , indicating that there existed some molecular interaction between PTX and HPMCAS. The interactions further contributed to the strong crystallization inhibition effect of HPMCAS toward PTX. The drug–polymer interaction in SD is speculated to occur via hydrogen bonding as the structure of HPMCAS-MF suggests several hydrogen bonding sites due to the OH and COOH functional groups provided by the acetyl and succinyl groups bound to the cellulose backbone.

Fig. 6 Transmission electron photomicrographs of **a** SD1 and **b** SD6. The corresponding electron diffraction patterns of **c** SD1 and **d** SD6

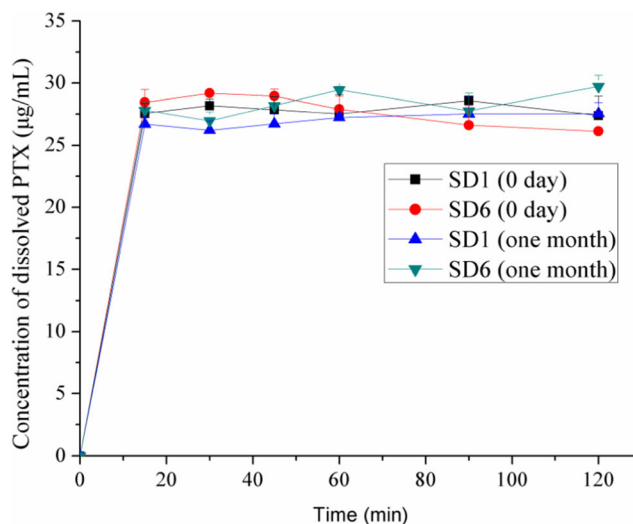
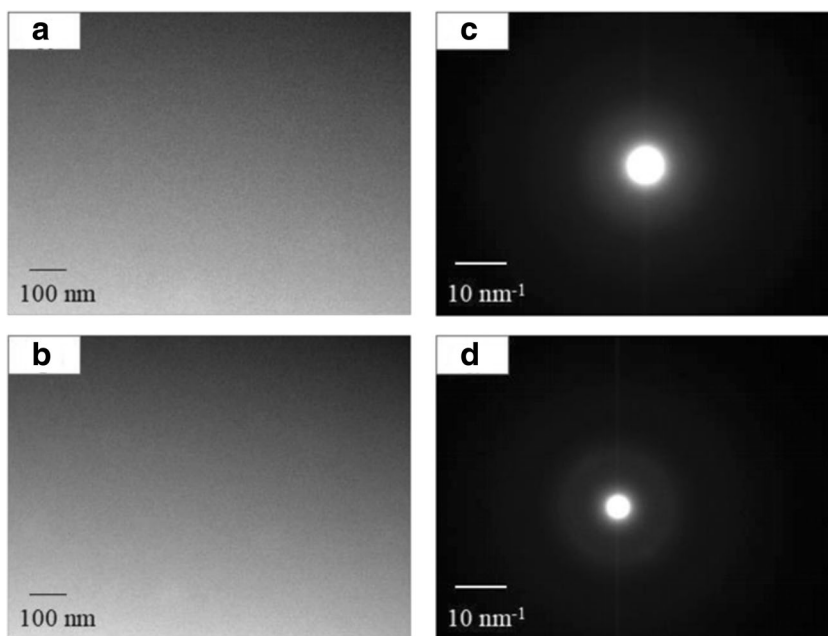


Fig. 7 Time profiles of in vitro dissolution of PTX from SD1 and SD6 on the 0th and 1 month after their preparation ($n = 3$)

TEM was used to examine the solid dispersions to evaluate the crystallinity and to further complement the DSC and XRD studies. Figure 6a, b shows TEM photomicrographs of SD1 and SD6. No distinct features were observed for the samples. The corresponding electron diffraction patterns of SD1 (c) and SD6 (d) do not exhibit sharp diffraction spots, indicating that PTX in the solid dispersions is amorphous.

Stability study

The results showed that the dissolution (Fig. 7) rate and extent of PTX from SD1 and SD4 after 1-month storage at 40 °C with 75% RH was almost unchanged compared with that on

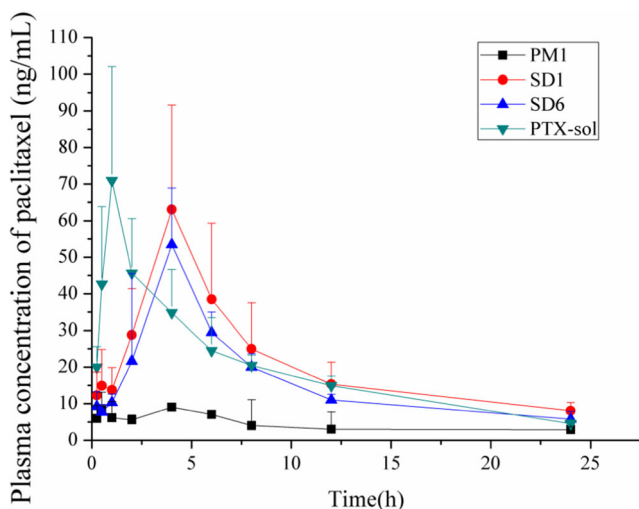


Fig. 8 Plasma concentration vs. time curves of PTX after oral administration of PTX-sol, PM1 (HPMCAS-MF/F68/PTX = 75:15:10), SD1 (HPMCAS-MF/F68/PTX = 75:15:10), and SD6 (HPMCAS/PTX = 90:10) at a dose of 20 mg/kg to rats ($n = 6$)

the 0th day. Also, the XRD and DSC outcomes (data not shown) of the SDs obtained before and after 1-month storage showed that PTX were at amorphous state. These indicated the acceptable physical stability of SD1 and SD6.

Pharmacokinetic evaluation

To assess whether the PTX solid dispersion had an absorption-enhancing effect, a pharmacokinetic evaluation was performed using Sprague-Dawley rats. As HPMCP, L100, HPMCAS-LF, and HPMCAS-HF could not maintain the supersaturation of PTX in the dissolution profiles, SD1 and SD6 were chosen to conduct the pharmacokinetic experiment. The mean plasma concentration-time profiles of PTX after oral administration of SDs, PM and PTX-sol at a dose of 20 mg/kg is shown in Fig. 8, and the relevant pharmacokinetic parameters are listed in Table 4. Compared with the PM1 group, SDs and PTX-sol groups significantly increased the AUC of PTX. It can be seen that SD6 and SD1 barely improved the oral bioavailability of PTX compared with PTX-sol with the exception that the appearance time of maximal plasma concentration was delayed due to the use of the enteric polymer. In vitro dissolution tests implied that 15% F68 had

no obvious effect on the dissolution, which coincided well with the in vivo oral absorption. Potentially, PTX-sol was able to induce supersaturation after contacting with the gastrointestinal fluid as long as the solubilization effect of Cremophor could be counteracted by increasing PTX concentration to the amorphous solubility. It was reported that Cremophor could inhibit P-gp in the small intestine to some extent and increase the bioavailability of orally administered P-gp substrate drugs [50]. For the solid dispersions, unsatisfactory outcomes may occur due to certain obstacles in vivo. It was demonstrated that LLPS would occur at a much higher concentration because of the solubilization by the solubilizing additives in the intestinal tract, such as lecithin and sodium taurocholate [45]. Even though the amorphous solid dispersion may dissolve rapidly in intestine, resulting in the formation of the drug-rich phase, the complex biological situation and other types of inner substances may disturb the equilibrium between the colloidal aggregates and the aqueous phase [51]. It was reported that additives had a great impact on the stability and size of the drug-rich phase, which further influenced the absorption and bioavailability of the drug [52]. In an ideal situation, the “reservoir” effect of the drug-rich phase has the advantage of enabling the passive transport of the drug across the intestinal membrane at a sustained state by rapidly replenishing drug that has been removed [53]. Perhaps, the carrier-mediated mechanisms account for the majority of the PTX transport process in oral absorption. Namely, there is still a gap between the supersaturation and the absorption, which may be altered by a higher supersaturation in vivo [32].

Conclusions

PTX solid dispersions were prepared through the solvent cast method in order to improve the oral bioavailability of PTX through supersaturation. The enteric polymer HPMCAS-MF was shown to be superior to other tested polymers for its ability to inhibit crystallization and maintain supersaturation of PTX for a long time in vitro. However, pharmacokinetic evaluation of SDs performed in rats did not show the advantages and increase the oral bioavailability of PTX compared with the PTX-sol. Perhaps, a higher supersaturation is needed to increase the oral absorption of BCS IV drugs using solid dispersions.

Table 4 Pharmacokinetic parameters of PTX after oral administration of PTX-sol, PTX-PM1 (HPMCAS-MF/F68/PTX = 75:15:10), PTX-SD1 (HPMCAS-MF/F68/PTX = 75:15:10), and SD6 (HPMCAS, PTX = 90:10) at a dose of 20 mg/kg ($n = 6$)

Parameter	SD1	SD6	PTX-sol	PM1
AUC _{0-∞} (μg/L*h)	592.8 ± 164.0	406.7 ± 57.8	520.4 ± 104.8	332.6 ± 193.1
T _{max} (h)	3.3 ± 1.0	3.6 ± 0.9	0.9 ± 0.2	4.2 ± 1.3
C _{max} (μg/L)	67.9 ± 22.1	56.6 ± 15.4	71.3 ± 31.2	14.4 ± 5.0
F (%)	178	122	156	100

Funding information This work was supported by the National Basic Research Program of China (973 Program, No. 2015CB932103), National Natural Science Foundation of China (No. 81673378), and China Postdoctoral Science Foundation (2016M600216).

Compliance with ethical standards

Conflict of interest The authors declare that they have no conflict of interest.

Ethical approval All institutional and national guidelines for the care and use of laboratory animals were followed.

References

- Battle JF, et al. Oral chemotherapy: potential benefits and limitations. *Rev Oncol*. 2004;6(6):335–40.
- Rao VM, Stella VJ. When can cyclodextrins be considered for solubilization purposes? *J Pharm Sci*. 2003;92(5):927–32.
- Dahan A, Beig A, Lindley D, Miller JM. The solubility-permeability interplay and oral drug formulation design: two heads are better than one. *Adv Drug Deliv Rev*. 2016;101:99–107.
- Dahan A, Miller JM. The solubility-permeability interplay and its implications in formulation design and development for poorly soluble drugs. *Aaps J*. 2012;14(2):244–51.
- Green MC, Buzdar AU, Smith T, Ibrahim NK, Valero V, Rosales MF, et al. Weekly paclitaxel improves pathologic complete remission in operable breast cancer when compared with paclitaxel once every 3 weeks. *J Clin Oncol Off J Am Soc Clin Oncol*. 2005;23(25):5983–92.
- Rowinsky EK, et al. Taxol: the first of the taxanes, an important new class of antitumor agents. *Semin Oncol*. 1992;19(6):646.
- Brouwers J, Brewster ME, Augustijns P. Supersaturating drug delivery systems: the answer to solubility-limited oral bioavailability? *J Pharm Sci*. 2009;98(8):2549–72.
- Mo R, Jin X, Li N, Ju C, Sun M, Zhang C, et al. The mechanism of enhancement on oral absorption of paclitaxel by N-octyl-O-sulfate chitosan micelles. *Biomaterials*. 2011;32(20):4609–20.
- Feng SS, Zhao L, Zhang Z, Bhakta G, Yin Win K, Dong Y, et al. Chemotherapeutic engineering: vitamin E TPGS-emulsified nanoparticles of biodegradable polymers realized sustainable paclitaxel chemotherapy for 168h in vivo. *Chem Eng Sci*. 2007;62(23):6641–8.
- Wang XX, et al. The antitumor efficacy of functional paclitaxel nanomicelles in treating resistant breast cancers by oral delivery. *Biomaterials*. 2011;32(12):3285.
- Lv PP, Wei W, Yue H, Yang TY, Wang LY, Ma GH. Porous quaternized chitosan nanoparticles containing paclitaxel nanocrystals improved therapeutic efficacy in non-small-cell lung cancer after oral administration. *Biomacromolecules*. 2011;12(12):4230–9.
- Liu F, Park JY, Zhang Y, Conwell C, Liu Y, Bathula SR, et al. Targeted cancer therapy with novel high drug-loading nanocrystals. *J Pharm Sci*. 2010;99(8):3542–51.
- Lee E, Lee J, Lee IH, Yu M, Kim H, Chae SY, et al. Conjugated chitosan as a novel platform for oral delivery of paclitaxel. *J Med Chem*. 2008;51(20):6442–9.
- Jain S, Kumar D, Swarnakar NK, Thanki K. Polyelectrolyte stabilized multilayered liposomes for oral delivery of paclitaxel. *Biomaterials*. 2012;33(28):6758–68.
- Mazzafarro S, Bouchemal K, Ponchel G. Oral delivery of anticancer drugs I: general considerations. *Drug Discov Today*. 2013;18(1–2):25–34.
- Roger E, Lagarce F, Garcion E, Benoit JP. Lipid nanocarriers improve paclitaxel transport throughout human intestinal epithelial cells by using vesicle-mediated transcytosis. *J Control Release*. 2009;140(2):174–81.
- Batrakova EV, Han HY, Alakhov VY, Miller DW, Kabanov AV. Effects of pluronic block copolymers on drug absorption in Caco-2 cell monolayers. *Pharm Res*. 1998;15(6):850–5.
- Sue May L, et al. Enhancement of docetaxel solubility using binary and ternary solid dispersion systems. *Drug Dev Ind Pharm*. 2015;41(11):1.
- Warren DB, Benameur H, Porter CJH, Pouton CW. Using polymeric precipitation inhibitors to improve the absorption of poorly water-soluble drugs: a mechanistic basis for utility. *J Drug Target*. 2010;18(10):704–31.
- Seeballuck F, Ashford MB, O'Driscoll CM. The effects of pluronics block copolymers and Cremophor EL on intestinal lipoprotein processing and the potential link with P-glycoprotein in Caco-2 cells. *Pharm Res*. 2003;20(7):1085–92.
- Curatolo W, Nightingale JA, Herbig SM. Utility of hydroxypropylmethylcellulose acetate succinate (HPMCAS) for initiation and maintenance of drug supersaturation in the GI milieu. *Pharm Res*. 2009;26(6):1419–31.
- Sawicki E, Schellens JHM, Beijnen JH, Nuijen B. Inventory of oral anticancer agents: pharmaceutical formulation aspects with focus on the solid dispersion technique. *Cancer Treat Rev*. 2016;50:247–63.
- Amidon GL, Lennemäs H, Shah VP, Crison JR. A theoretical basis for a biopharmaceutic drug classification: the correlation of in vitro drug product dissolution and in vivo bioavailability. *Pharm Res*. 1995;12(3):413–20.
- Rabizzoni P. Development of a rebamipide solid dispersion system with improved dissolution and oral bioavailability. *Arch Pharm Res*. 2015;38(4):522.
- Shuai S, Yue S, Huang Q, Wang W, Yang J, Lan K, et al. Preparation, characterization and in vitro/vivo evaluation of tectorigenin solid dispersion with improved dissolution and bioavailability. *Eur J Drug Metab Pharmacokin*. 2016;41(4):413–22.
- Miller JM, Beig A, Carr RA, Spence JK, Dahan A. A win-win solution in oral delivery of lipophilic drugs: supersaturation via amorphous solid dispersions increases apparent solubility without sacrifice of intestinal membrane permeability. *Mol Pharm*. 2012;9(7):2009–16.
- Beig A, Fine-Shamir N, Lindley D, Miller JM, Dahan A. Advantageous solubility-permeability interplay when using amorphous solid dispersion (ASD) formulation for the BCS class IV P-gp substrate Rifaximin: simultaneous increase of both the solubility and the permeability. *Aaps J*. 2017;19(3):806–13.
- Blandizzi C, Viscomi GC, Scarpignato C. Impact of crystal polymorphism on the systemic bioavailability of rifaximin, an antibiotic acting locally in the gastrointestinal tract, in healthy volunteers. *Drug Des Devel Ther*. 2014;9:1–11.
- Walle UK, Walle T. Taxol transport by human intestinal epithelial Caco-2 cells. *Drug Metab Dispos*. 1998;26(4):343.
- Sandström M, et al. The pharmacokinetics of epirubicin and docetaxel in combination in rats. *Cancer Chemother Pharmacol*. 1999;44(6):469–74.
- Peltier S, Oger JM, Lagarce F, Couet W, Benoît JP. Enhanced oral paclitaxel bioavailability after administration of paclitaxel-loaded lipid nanocapsules. *Pharm Res*. 2006;23(6):1243–50.
- Artursson P. Coexistence of passive and carrier-mediated processes in drug transport. *Nat Rev Drug Discov*. 2010;9(8):597–614.
- Abuasal BS, Bolger MB, Walker DK, Kaddoumi A. In silico modeling for the nonlinear absorption kinetics of UK-343,664: a P-gp and CYP3A4 substrate. *Mol Pharm*. 2012;9(3):492–504.
- Cisternino S, Bourasset F, Archimbaud Y, Sémioud D, Sanderink G, Scherrmann JM. Nonlinear accumulation in the brain of the new

- taxoid TXD258 following saturation of P-glycoprotein at the blood-brain barrier in mice and rats. *Br J Pharmacol.* 2003;138(7):1367–75.
35. Varma MVS, Khandavilli Sateesh A, Panchagnula R. Functional role of P-glycoprotein in limiting intestinal absorption of drugs: contribution of passive permeability to P-glycoprotein mediated efflux transport. *Mol Pharm.* 2005;2(1):12–21.
 36. Moes J, Koolen S, Huitema A, Schellens J, Beijnen J, Nuijen B. Development of an oral solid dispersion formulation for use in low-dose metronomic chemotherapy of paclitaxel. *Eur J PharmBiopharm.* 2013;83(1):87–94.
 37. Huizing MT, Rosing H, Koopman F, Keung ACF, Pinedo HM, Beijnen JH. High-performance liquid chromatographic procedures for the quantitative determination of paclitaxel (Taxol) in human urine. *J Chromatogr B Biomed Appl.* 1995;664(2):373–82.
 38. Piao H, et al. A pre-formulation study of a polymeric solid dispersion of paclitaxel prepared using a quasi-emulsion solvent diffusion method to improve the oral bioavailability in rats. *Drug Dev Ind Pharm.* 2016;42(3):1–11.
 39. Ilevbare GA, Taylor LS. Liquid–liquid phase separation in highly supersaturated aqueous solutions of poorly water-soluble drugs: implications for solubility enhancing formulations. *Cryst Growth Des.* 2013;13(4):1497–509.
 40. Jackson MJ, Toth SJ, Kestur US, Huang J, Qian F, Hussain MA, et al. Impact of polymers on the precipitation behavior of highly supersaturated aqueous danazol solutions. *Mol Pharm.* 2014;11(9):3027–38.
 41. Chen Y, et al. Sodium lauryl sulphate competitively interacts with HPMC-AS and consequently reduces oral bioavailability of posaconazole/HPMC-AS amorphous solid dispersion. *Mol Pharm.* 2016;13(8)
 42. Ueda K, Higashi K, Moribe K. Direct NMR monitoring of phase separation behavior of highly supersaturated Nifedipine solution stabilized with Hypromellose derivatives. *Mol Pharm.* 2017;14(7):2314–22.
 43. Ilevbare GA, Liu H, Pereira J, Edgar KJ, Taylor LS. Influence of additives on the properties of nanodroplets formed in highly supersaturated aqueous solutions of ritonavir. *Mol Pharm.* 2013;10(9):3392–403.
 44. Ilevbare GA, et al. Effect of binary additive combinations on solution crystal growth of the poorly water-soluble drug, *Ritonavir*. *Cryst Growth Des.* 2017;12(12):6050–60.
 45. Raina SA, Zhang GGZ, Alonzo DE, Wu J, Zhu D, Catron ND, et al. Impact of solubilizing additives on supersaturation and membrane transport of drugs. *Pharm Res.* 2015;32(10):3350–64.
 46. Sun DD, Lee PI. Evolution of supersaturation of amorphous pharmaceuticals: the effect of rate of supersaturation generation. *Mol Pharm.* 2013;10(11):4330–46.
 47. Lahav M, Leiserowitz L. The effect of solvent on crystal growth and morphology. *Chem Eng Sci.* 2001;56(7):2245–53.
 48. Prasad D, Chauhan H, Atef E. Role of molecular interactions for synergistic precipitation inhibition of poorly soluble drug in supersaturated drug-polymer-polymer ternary solution. *Mol Pharm.* 2016;13(3):756–65.
 49. Puel F, Verdurand E, Taulelle P, Bebon C, Colson D, Klein JP, et al. Crystallization mechanisms of acicular crystals. *J Cryst Growth.* 2008;310(1):110–5.
 50. Tomaru A, Takeda-Morishita M, Maeda K, Banba H, Takayama K, Kumagai Y, et al. Effects of Cremophor EL on the absorption of orally administered saquinavir and fexofenadine in healthy subjects. *Drug Metab Pharmacokinet.* 2015;30(3):221–6.
 51. Taylor LS, Zhang GG. Physical chemistry of supersaturated solutions and implications for oral absorption. *Adv Drug Deliv Rev.* 2016;101:122–42.
 52. Frenkel YV, Clark AD, Das K, Wang YH, Lewi PJ, Janssen PAJ, et al. Concentration and pH dependent aggregation of hydrophobic drug molecules and relevance to oral bioavailability. *J Med Chem.* 2005;48(6):1974–83.
 53. Indulkar AS, Gao Y, Raina SA, Zhang GGZ, Taylor LS. Exploiting the phenomenon of liquid–liquid phase separation for enhanced and sustained membrane transport of a poorly water-soluble drug. *Mol Pharm.* 2016;13(6):2059–69.